Reviewer # 1 Questions and our responses

We thank Reviewer #1 for constructive comments and suggestions to improve our paper. In this section, we first list reviewer's questions/comments, and then provide our answers. The questions/comments are in italics, and our responses are in bold text.

In this paper, the authors proposed an unsteady analytical model for salt intrusion to understand the spatial-temporal dynamics of salt transport under different riverine and tidal forcing. The model was applied to the Humen estuary, which is a tide-dominated and well-mixed estuary. And the modelled results correspond well with the observed data. The paper is interesting and of important scientific implications for estuarine dynamics. However, there are still some major concerns that should be properly addressed before the paper can be accepted in this journal. Thus, I would suggest the authors to have a substantial revision.

Major concerns:

1. Method in Section 2: It is noted that a rather similar approach for salinity intrusion in an unsteady state was proposed by Song et al. (2008) entitled "One-dimensional unsteady analytical solution of salinity intrusion in estuaries". It is better to clarify the main difference between the current model and the one proposed by Song et al. (2008) in order to highlight the new insights into the salt dynamics.

The unsteady analytical model developed by Song et al. (2008) can reproduce the salinity process in an idealized estuary with constant depth and constant width. Song's model is thus applicable to laboratory flumes and artificial channels. However, the channel cross-sectional area of estuaries is typically converging. One innovation of our paper is to better capture the natural topography of alluvial estuaries, assuming the cross-sectional area to obey an exponential function. So, our paper continues on Song's work within the geometrical setting of an alluvial estuary. We will clarify this in the revision.

Song, Z. Y., Huang, X. J., Zhang, H. G., Chen, X. Q., and Kong, J.: One–dimensional unsteady analytical solution of salinity intrusion in estuaries, China Ocean Eng., 22, 113–122, 2008.

2. P8, Lines 19-24, estimation of the tidal excursion: Note that the tidal excursion is a critical parameter that links the salinity intrusion to the tidal hydrodynamics. In this study, the authors assumed that the longitudinal tidal excursion can be described an exponential function. However, such an assumption is only reasonable for a short channel (Let's say less than 10 km). I would suggest the authors to adopt an analytical hydrodynamics model to reproduce the longitudinal tidal excursion since there exists a long traditional analytical solution for tidal hydrodynamics in estuaries (e.g., Toffolon and Savenije, 2011; Winterwerp and Wang, 2013; Cai et al., 2016). The advantage of coupling the salinity intrusion model to the tidal dynamics lies in that it enables directly linking the salt dynamics into the tidal forcing (e.g., tidal amplitude imposed at the estuary mouth). Moreover, it allows to have a prediction of salinity intrusion for

different tidal forcing conditions (e.g., neap-spring changes) for given tidal amplitude observed at the estuary mouth. The current model used the observed salinity to forecast the tidal excursion (i.e., Eq. 18 in the manuscript), which is not very practical if prediction is required.

We appreciate the reviewer's suggestion and will use an analytical model for tidal hydrodynamics to compute the excursion length in the revised version. In the Method section, we will introduce Cai's method (Cai et al., 2016) as below:

"Tidal wave propagation can be described analytically by a set of four implicit equations (Cai et al., 2012), the phase lag equation $\tan(\varepsilon)=\lambda/(\gamma-\delta)$**, the scaling equation** $\mu=\sin(\varepsilon)/\lambda$**, the damping equation** $\delta=\gamma/2-4\chi\mu/(9\pi\lambda)-\chi\mu^2/3$**, and the celerity equation** $\lambda^2=1-\delta(\lambda-\delta)$**, where λ is the celerity number** $\lambda=c_0/c$**, μ is the velocity number** $\mu=\upsilon\bar{h}/(r_s\eta c_0)$**, δ is the damping number** $\delta=c_0\mathrm{d}\eta/(\eta\mathrm{d}x\omega)$**, and ε is the phase lag between HW and HWS** $\varepsilon=\pi/2-(\phi_Z-\phi_U)$**. Here, three dimensionless parameters control the tidal hydrodynamics (Savenije et al., 2008), i.e. the dimensionless tidal amplitude** $\zeta=\eta/\bar{h}$**, the estuary shape number** $\gamma=c_0/(\omega a)$ **and the friction number** $\chi=r_s g c_0\zeta/\left(K_s^2\omega\bar{h}^{4/3}\right)\left[1-(4\zeta/3)^2\right]^{-1}$**, where η is the tidal amplitude, K_S is the Manning-Strickler friction coefficient, r_s the storage width ratio,** $\bar{h}$ **is the tide-averaged depth and c_0 is the classical wave celerity** $c_0=\sqrt{g\bar{h}/r_s}$**. Then, with the available geometry and friction data at the estuary mouth, the tidal propagation celerity and the tidal amplitude (or the tidal excursion) can be obtained by solving the set of four equations."**

In addition, we will apply the hydrodynamics model proposed by Cai et al. (2016) to the Humen estuary based on observations. The averaged depth along the axis of the Humen estuary is shown in Figure S1. The coefficient of determination R^2 is 0.67, which indicates that the topography is too complex to be represented by an exponential function. The water depth is influenced greatly by human activities. The input parameters used for the tidal hydrodynamics model will be summarized in Table S1. A new Figure S2a shows the computed tidal amplitude and the tidal excursion obtained with a hybrid model, using a variable depth along the estuary (Cai et al., 2012). The tidal amplitude along the Humen estuary can be well simulated by the analytical model while the tidal excursion is underestimated. There are two reasons which may cause the underestimation. The first one is due to the inaccurate estimation of the averaged depth along the estuary, since the depth convergence length *d* cannot be fitted well to the exponential function $\bar{h}=\bar{h}_0\exp(x/-d)$ **in the Humen estuary. It can have a serious impact on the three dimensionless parameters which control the tidal hydrodynamics, i.e. the dimensionless tidal amplitude, the estuary shape number and the friction number. The other one is the assumption that the tidal excursion is independent of the distance along the Humen estuary. Well, as was shown by Savenije (2005), the tidal excursion can be assumed to be constant in many estuaries worldwide. However, a conclusion from the measurement data show that the tidal excursion may be damped along the estuary, like in the Mekong Estuary. In four estuary branches, over more than 100 kilometers, tidal excursion decay can be described by an**

exponential function (Nguyen, 2008). In Figure S3a we will present the computed salinity curves using the calibrated variable tidal excursion along the Humen estuary. It better reproduces the salinity at HWS and LWS compared with the results obtained based on a hybrid model shown in Figure S3b. Therefore, similarly, the observations in the Humen estuary indicate that the tidal excursion decreases exponentially.

We agree with the reviewer that it is important to link the salinity intrusion to the tidal hydrodynamics. It can help the model to become applicable to a wider range of flow conditions. Therefore, the analytical hydrodynamics model by Cai et al. (2012) will be presented in the revised methods section. We will offer an analytical approach to reproduce the main tidal dynamics coupling to the salt dynamics. However, unfortunately, the analytical model for tidal dynamics cannot be used in this case, due to the limitations of available geometry as well as the assumption of the tidal excursion. So, in Section 4, we will provide another way to calibrate the tidal excursion based on the measurements of salinity.

Cai, H., Savenije, H. H. G., and Toffolon, M.: A new analytical framework for assessing the effect of sea-level rise and dredging on tidal damping in estuaries, J. Geophys. Res., 117, C09023, doi:10.1029/2012JC008000, 2012.

Cai, H., Toffolon, M., and Savenije, H.H.G.: An analytical approach to determining resonance in semi-closed convergent tidal channels, Coast Eng. J., 58(03), 1650009, 2016.

Nguyen, A. D.: Salt Intrusion, Tides and Mixing in Multi-Channel Estuaries: PhD: UNESCO-IHE Institute, Delft. CRC Press, 2008, p52.

Savenije, H. H. G.: Salinity and Tides in Alluvial Estuaries, Elsevier, Amsterdam, 2005.

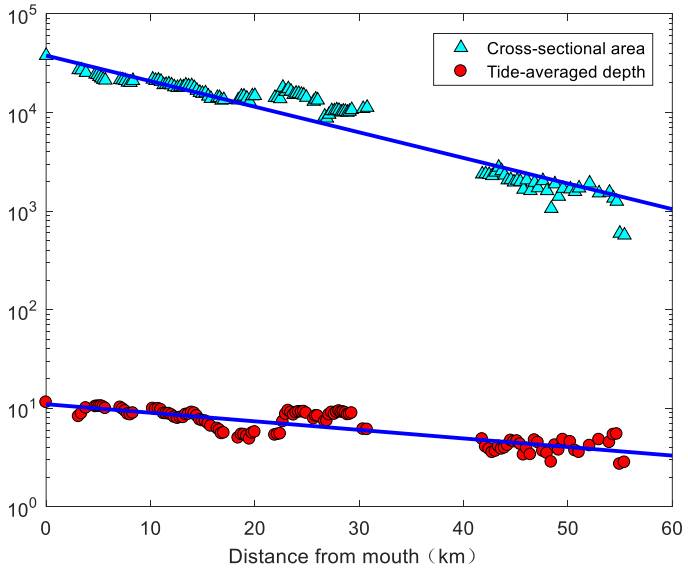

Figure S1: Shape of the Humen estuary, showing the correlation between the cross-sectional area A (m^2) and averaged depth $\bar{h}$ along the estuary axis with fitted trend lines.

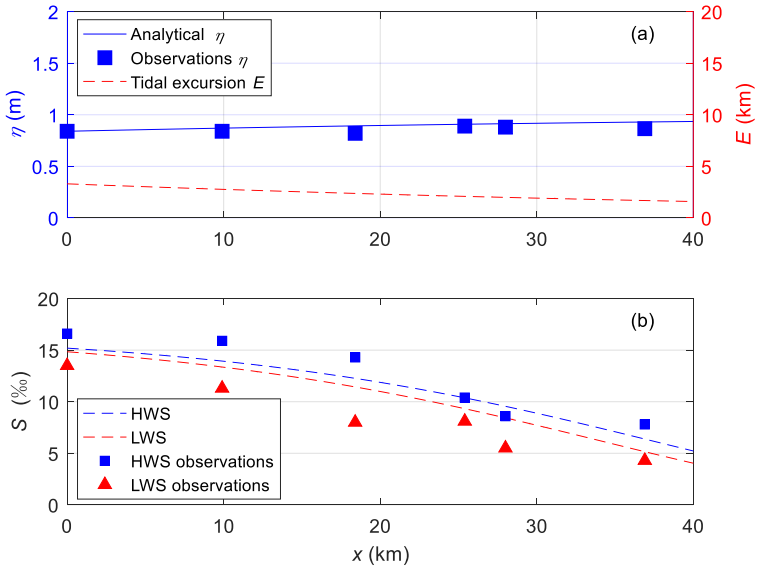

Figure S2: (a) The computed tidal amplitude and tidal excursion in the Humen estuary based on a hybrid model using a variable depth along the estuary; (b) Comparison between computed salinity and the observations at HWS and LWS. The tidal excursion is computed with a hybrid model.

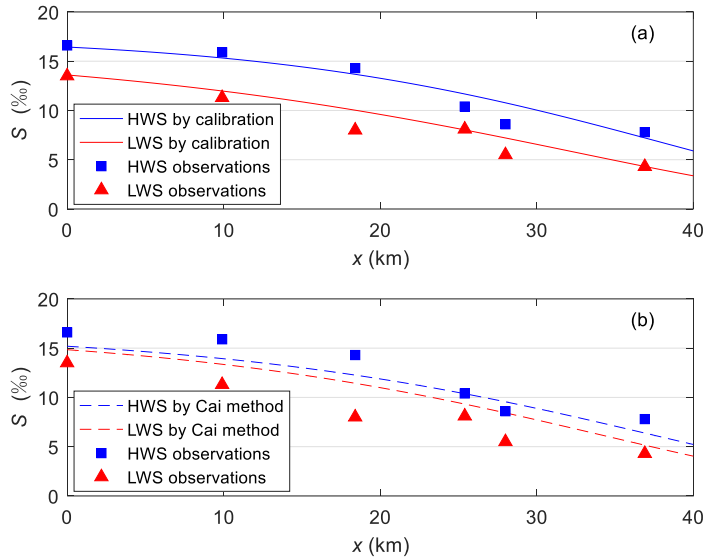

Figure S3: (a) Comparison between the observed and computed salinity curve using the calibrated tidal excursion; (b) Comparison between the observed and computed salinity curve based on a hybrid model using a variable depth along the estuary.

Table S1: Inputs used for the tidal hydrodynamics model

	A (m^2)	a (km)	h_0 (m)	d (km)	η_0 (m)	Ks ($m^{1/3}s^{-1}$)	T (s)	s_0 (‰)
Humen	**37822**	**16.7**	**10**	**50**	**0.84**	**35**	**44400**	**15.02**

3. P8, Lines 25-29, estimation of the wave celerity: Similar to the tidal excursion, I would suggest the authors to link the wave celerity to the tidal forcing imposed at the estuary mouth by means of an analytical model for tidal hydrodynamics.

The analytical hydrodynamics model (Cai et al., 2012) will be presented in the method section in the revised version, but it does not apply to our specific field case.

Cai, H., Savenije, H. H. G., and Toffolon, M.: A new analytical framework for assessing the effect of sea-level rise and dredging on tidal damping in estuaries, J. Geophys. Res., 117, C09023, doi:10.1029/2012JC008000, 2012.

4. For the time being, the authors only illustrate the proposed analytical model applied to the Humen estuary during the neap tide condition, when the salt intrusion length is approximately minimum. I would suggest the authors to adopt the model to the case during the spring tide condition when the salt intrusion really matters. In section 4.2 concerning the model validation, since the authors only used the dataset from Jan. 29th to Feb. 3rd, I think this is only kind of the model calibration rather than validation because the tidal hydrodynamics is more or less the same during the chosen period.

In the study, the salinity is assumed to be forced by a harmonic tidal wave with a single-frequency. So our model is more applicable for estuaries with semidiurnal tides or diurnal tides. It is found that the semidiurnal tide is the distinctively dominant tidal wave in the neap tide in Humen, while the diurnal tide is as important as the semidiurnal tide in the spring tide. Therefore, we chose the data during the neap tide to illustrate our unsteady model in this case.

We have rewritten Section 4 to make it clearer in the revised version. The calibrated parameters include tidal excursion *E* and dispersion coefficient *D*. Although each of the calibrated dispersion coefficients from 29 January to 3 February was listed in Table 2, in fact, only the one on 29 January was used for calibration. In other words, we use the data on 29 January to calibrate the parameters of the model and use the data from 30 January to 3 February to validate the model. To make it clearer, in the revised version, we use two figures to show the results, Figure 4 is the calibrated result and Figure 5 is the validation results, as below:

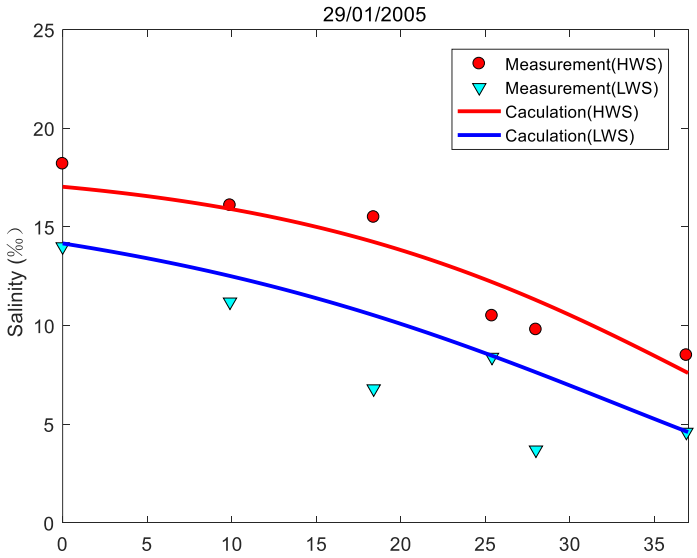

Figure 4: Comparison between calibration result and measured salinity concentration along the river on 29 January, 2005, showing values of measured salinity at high water slack (circle) and low water slack (inverted triangle), and the calibrated salinity curves at high water slack (red curve) and low water slack (blue curve).

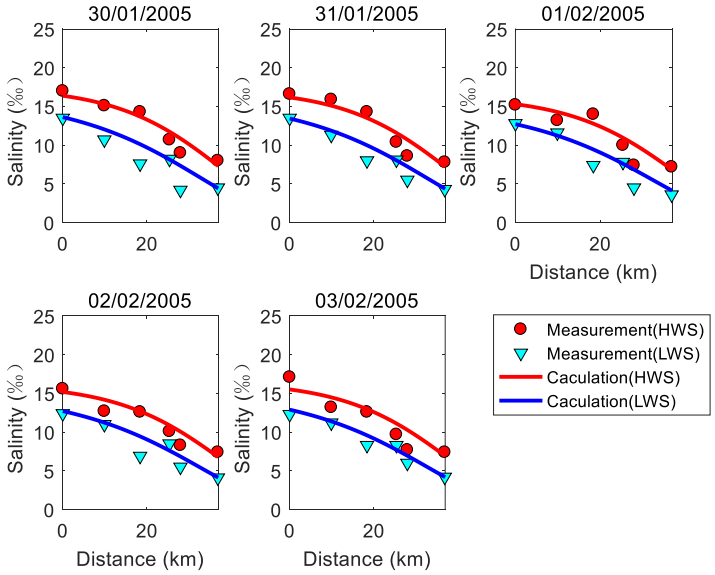

Figure 5: Comparison between validation result and measured salinity concentration along the river from 30 January to 3 February, 2005.

5. Sensitivity analysis: As mentioned by the authors, the proposed analytical model can directly reflect the influence of the tide and the interaction between the tide and runoff (see Abstract part in Line 17). Hence, it is better to conduct a sensitivity analysis of the salinity distribution to both the tidal and riverine forcing imposed at both ends of the estuary.

We appreciate the reviewer's suggestion and add a "Sensitivity analysis" part in the revised version, as below:

"The amplitude of salinity can be described by:

$$\hat{s} = \overline{s}_x * I_s \text{,} \quad \textbf{(23)}$$

where $\overline{s}_x$ is the tide-averaged salinity along the estuary and is a function of the river discharge, i.e. Eq.(12). The parameter I_s is the salinity amplitude coefficient that is defined as:

$$I_s = -\frac{EQ_f}{2DA} \text{,} \quad \textbf{(24)}$$

representing the interaction between the tides and the river discharge. To investigate the longitudinal salinity distribution and intratidal salinity variation for different discharge and tidal dynamic conditions in the Humen estuary, Eqs. (12) and (23) are used to plot the longitudinal salinity curve and intratidal variation of salinity, respectively. The implemented parameters are the same as shown in Table 3, only the river discharge and the tidal excursion are variable.

Three constant discharge values of 200, 600 and 1800 m^3/s are used to evaluate the impact of the river discharge on the salinity variation. The discharges are chosen because the minimum discharge in the dry season is around 600 m^3/s in the Humen estuary, and low salinity can be measured at Huangpuyou station when the discharge is larger than 1800 m^3/s. In addition, the discharge in the extreme dry season is set to be 200 m^3/s. The longitudinal salinity curve can be seen Figure 9a. At tidal average conditions, the salt intrusion length gets smaller when the discharge increases. The steepest salinity gradient can be found at the highest discharge (Q_f=1800 m^3/s). It is clear from Figure 9b that the salinity amplitude increases firstly and then decreases as the river discharge increases. This is because during periods of low river discharge (Q_f= 200 m^3/s), the tide-averaged salinity is larger but the salinity amplitude coefficient I_s is smaller, which indicates the weaker interaction between the river flow and the tides. However, the tide-averaged salinity decreases rapidly with the increasing river discharge as we can see from Figure 9a, resulting in a smaller amplitude of salinity during periods of high river discharge (Q_f= 1800 m^3/s).

The tidal effect is studied using three different tidal excursions. The tidal excursion values result in the plots that is shown in Figure 10. The longitudinal salinity distribution at tidal average conditions is independent of the tidal excursion, as can be seen in Figure 10a. From Eq. (23), since the salinity amplitude coefficient I_s is in direct proportion to the tidal excursion, the amplitude of the salinity shows a linearly increasing trend with the increased tidal excursion (Figure 10b)."

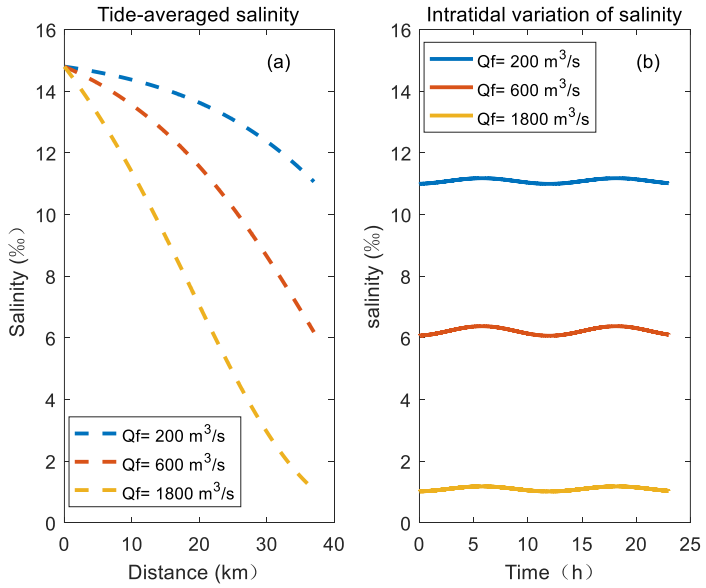

Figure 9: (a) Longitudinal salt intrusion curve at Tidal average considering different river discharge; (b) intratidal variation of salinity at Huangpuyou station on 31 January, 2005 considering different river discharge.

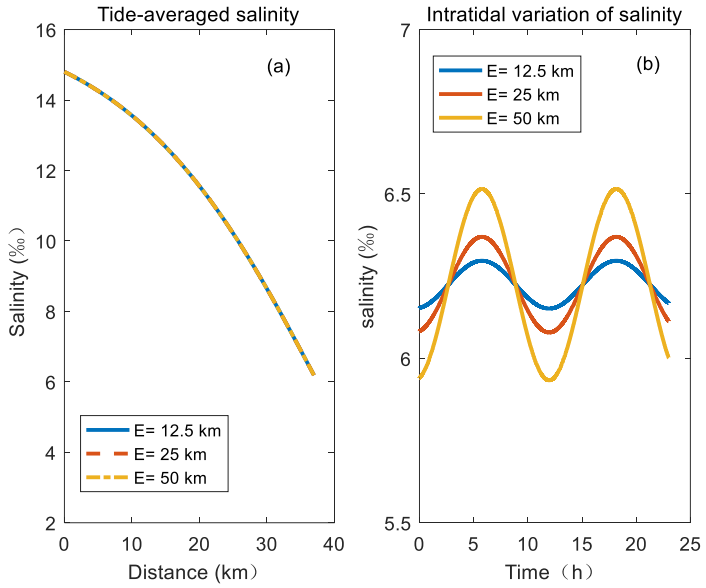

Figure 10: (a) Longitudinal salt intrusion curve at Tidal average considering different tidal excursion; (b) intratidal variation of salinity at Huangpuyou station on 31 January, 2005 considering different tidal excursion.

Minor concerns:

1. P3, Eq. (3) and Eq. (4): Here please clarify the physical meaning of s1 and s2 coefficients. In addition, it is noted that the salinity and velocity are assumed to be in phase since they have the same initial phase, am I right? Please also clarify this important assumption.

In fact, Eq. (3) is the expression of salinity using a first-order Fourier expansion method. Therefore, mathematically, s1 and s2 are the Fourier

expanding coefficients, and the physical meaning is the amplitude of salinity variation. Since the value of the initial phase in Eq. (3) has no impact on the Fourier expansion, we assume the salinity having the same initial phase with the velocity for convenience of calculating.

2. P7, Line 18: Please clarify where the salinity was sampled. It was sampled in the central part of the channel or near side banks? Due to the fact that the model used the cross-sectional averaged salinity concentration, it would be better to clarify this point.

Considering the impact of the shipping, the measuring positions were near the banks, with certain distances ranging from 605 m to 70 m.

3. P9, Lines 14-16: It is better to illustrate the stratification or mixing during the studied period since the authors already collected both the surface and bottom salinity concentration.

The field survey was carried out by Guangdong Province Hydrology Bureau and the Pearl Hydrology Bureau from the River Conservancy Commission. Unfortunately, they only provided us the vertically averaged salinity at each measuring location, related to the well-mixed condition in Humen estuary. For lack of the vertical salinity data, we further support this view in the revised version, as below:

"…The Humen estuary is well-mixed under normal flow conditions during the dry season (Ou, 2009; Luo et al., 2010). Due to three year's drought, the river discharge decreased by 30 to 50 percent during the study period in 2005 compared to a normal year (Liao, Pan, and Dong, 2008). Thus, it was well mixed during the calibration and validation…"

Liao, D.Y.; Pan, T.J., and Dong, Y.L., 2008. Characteristics of salt intrusion and its impact analysis in Guangzhou. Environment, S1, 4-5. (In Chinese)

Luo, L., Chen, J., Yang, W., and Wang, D.X, 2010. An intensive saltwater intrusion in the pearl river delta during the winter of 2007–2008, J. Trop. Oceanogr., 6, 22-28. (In Chinese)

Ou, S.Y., 2009. Spatial difference about activity of saline water intrusion in the Pearl River Delta. Scientia Geographica Sinica, 29(1), 89-92. (In Chinese)

4. P11, Lines 6-8: Due to the assumptions of Eqs. (3)-(4), the extreme values of salinity appear when the tidal velocity is zero.

In physical terms, the tidal flow moves in the reversed direction just in the next tick when the tidal velocity turns into zero. At that moment, the salinity at the study site is the maximum or minimum value. Savenije (2005) also assumed that the maximum salinity is reached when tidal discharge is zero.

Savenije, H. H. G.: Salinity and Tides in Alluvial Estuaries, Elsevier, Amsterdam, 2005, p141.

5. Figure 1: Please use 'West River' and 'North River' instead of 'Xijiang River' and 'Beijiang River', respectively. Meanwhile, it is better to indicate the locations of outlets

that were mentioned in the main text.

We appreciate the reviewer's suggestion and redraw Figure 1 in the revised version as below:

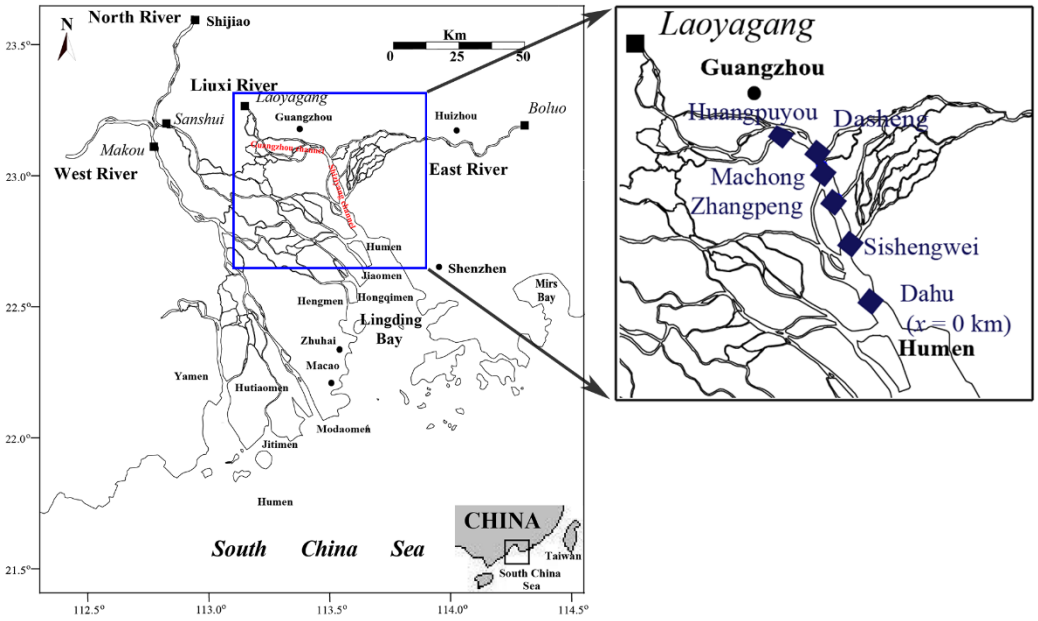

Figure 1: Map of the Humen estuary, showing the gauging stations where salinity concentration was measured during the field survey from 29 January to 3 February, 2005.

6. Figure 2: It is better to use the logarithm scale.

We will use a logarithmic scale in the revised version as below:

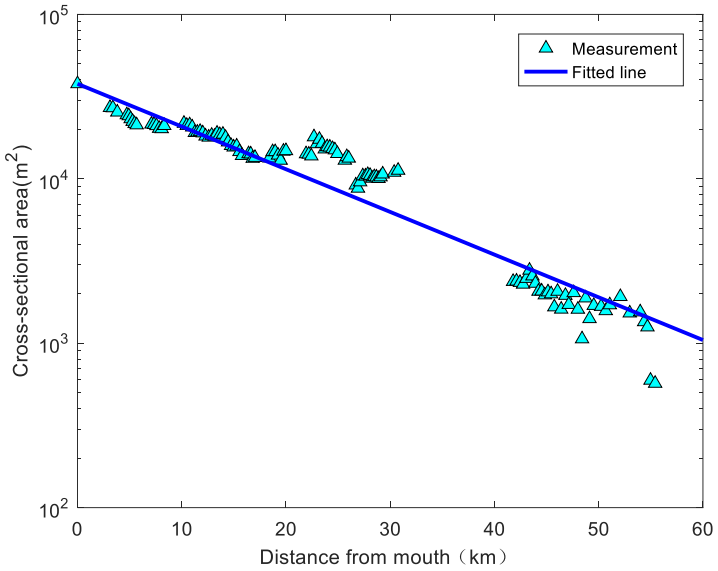

Figure 2: Shape of the Humen estuary, showing the correlation between the cross-sectional area A (m^2) and the distance from the estuary mouth x (km). The coefficient of determination R^2 is 0.92. The triangles represent observations and the line represents the fit to Eq. (1), where the area at the estuary mouth A_0=37822 m^2 and the area convergence length (a) is 16.7 km.

7. Figures 4, 6, 7: Please relocate the legend to a suitable place.

We appreciate the reviewer's suggestion and redraw Figures 4, 6 and 7 in the

revised version as below:

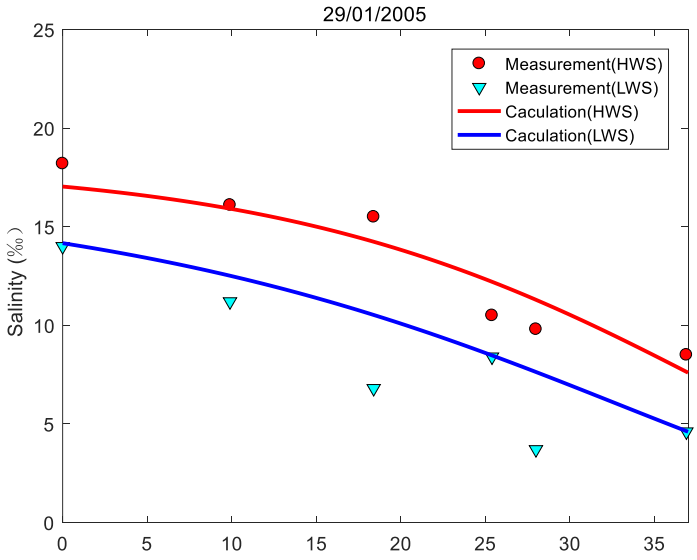

Figure 4: Comparison between calibration results and measured salinity concentration along the river on 29 January, 2005, showing values of measured salinity at high water slack (circles) and low water slack (inverted triangles), and the calibrated salinity curves at high water slack (red curve) and low water slack (blue curve).

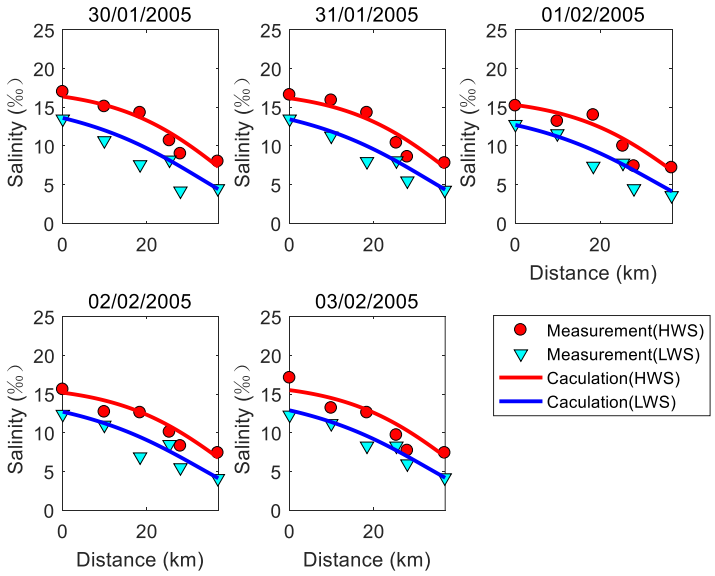

Figure 5: Comparison between validation result and measured salinity concentration along the river from 30 January to 3 February, 2005.

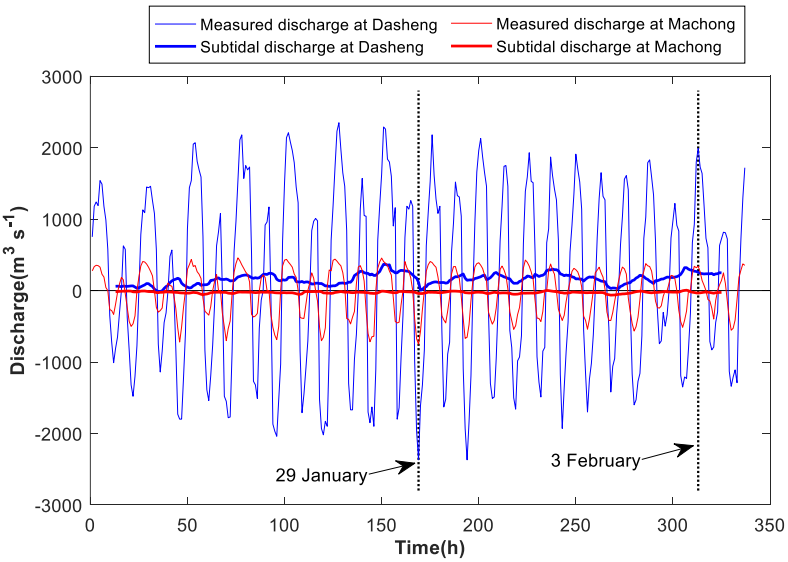

Figure 11: Subtidal discharge measured at Machong station and Dasheng station from 29 January through 3 February. Positive values mean seaward.

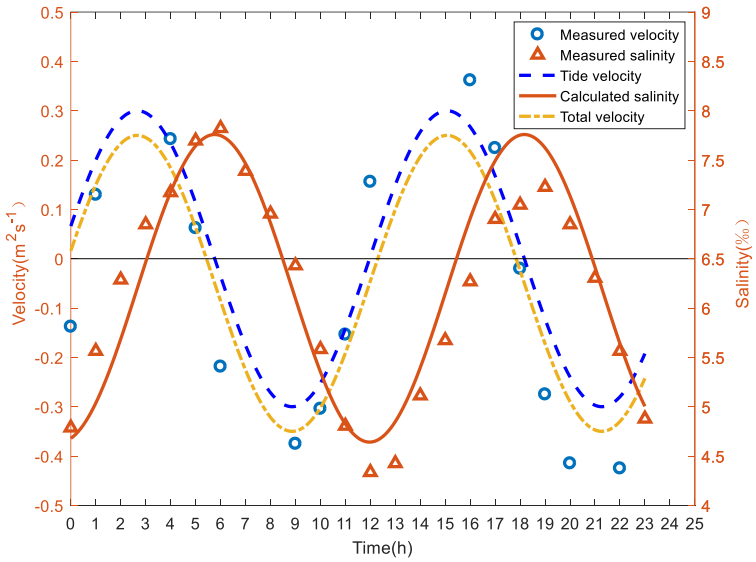

Figure 12: Salinity and tidal flow velocity over a tidal cycle at Huangpuyou station. The measured salinity is represented by triangles and the measured flow velocity is indicated by circles (on 31 January 2005). The dashes line is the calculated tidal velocity while the dash-dotted line is the total velocity of tidal flow and river flow. The red solid curve represents salinity simulated by the unsteady analytical solution, which reproduces the time lag HWS and maximum salinity.

References：

Cai, H., Toffolon, M., Savenije, H.H.G., 2016a. An analytical approach to determining resonance in semi-closed convergent tidal channels, Coast Eng. J., 58(03), 1650009.

Toffolon, M., Savenije, H.H.G., 2011. Revisiting linearized one-dimensional tidal propagation. J. Geophys Res., 116. DOI:ArtnC0700710.1029/2010jc006616

Winterwerp, J.C., Wang, Z.B., 2013. Man-induced regime shifts in small estuaries-I: theory. Ocean Dynam., 63(11-12): 1279-1292. DOI:10.1007/s10236-013-0662-9